

# Reliable measurement of the Li-like ${}^{48}_{22}\text{Ti } 1s2s2p {}^4P_{5/2}^0$ level lifetime by beam-foil and beam-two-foil experiments

T. Nandi,<sup>1,\*</sup> Nissar Ahmad,<sup>1,2</sup> A. A. Wani,<sup>2</sup> and P. Marketos<sup>3</sup><sup>1</sup>*Nuclear Science Center, Aruna Asaf Ali Marg, New Delhi 110 067, India*<sup>2</sup>*Department of Physics, Aligarh Muslim University, Aligarh 202 002, India*<sup>3</sup>*The Hellenic Open University, 6 Patriarchou Ioakeim Street, 106 74 Athens, Greece*

(Received 26 October 2005; published 21 March 2006)

We have determined the lifetime of the Li-like  ${}^{48}_{22}\text{Ti } 1s2s2p {}^4P_{5/2}^0$  level ( $210.5 \pm 13.5$  ps) using data from its x-ray decay channel through beam single- and two-foil experiments, coupled to a multicomponent iterative growth and decay analysis. Theoretical lifetime estimates for this zero-nuclear-spin ion lies within the uncertainty range of our experimental results, indicating that blending contributions to this level from the He-like  $1s2p {}^3P_2^0$  and  $1s2s {}^3S_1$  levels are eliminated within the current approach. A previously reported discrepancy between experimental and theoretical  $1s2s2p {}^4P_{5/2}^0$  level lifetimes in  ${}^{51}_{23}\text{V}$  may, as a result, be attributed to hyperfine quenching.

DOI: 10.1103/PhysRevA.73.032509

PACS number(s): 32.30.Rj, 32.70.Cs, 34.50.Fa

## I. INTRODUCTION

In a previous study [1] we have employed the beam single-foil [2] and beam two-foil techniques [3] coupled to an iterative multicomponent exponential growth and decay analysis, to address blending in lifetime measurements in He- and Li-like  ${}^{51}_{23}\text{V}$  ( $I=7/2$ ) levels. The experimental He-like V  $1s2p {}^3P_2^0$  [1] and  $1s2s {}^3S_1$  level lifetimes [4] are in good agreement with theoretical predictions [5], whereas the experimental Li-like V  $1s2s2p {}^4P_{5/2}^0$  level lifetime [1] is about 21% shorter than theoretical estimates [6–8] obtained without considering hyperfine quenching effects [9]. This trend is not, however, followed in other nonzero nuclear-spin ions. We note, for instance, that the experimental He-like Cl ( $I=3/2$ )  $1s2p {}^3P_2^0$  level lifetime ( $2.2 \pm 0.3$  ns, Ref. [10]) is in good agreement with the theoretical value (1.98 ns, Ref. [5]), whereas the Li-like Cl  $1s2s2p {}^4P_{5/2}^0$  level lifetime ( $0.95 \pm 0.2$  ns, Ref. [10],  $0.91 \pm 0.04$  ns, Ref. [11]) is larger than the theoretical prediction (0.81 ns, Ref. [12]). However, the experimental He-like Cl  $1s2s {}^3S_1$  level lifetime ( $280 \pm 25$  ns) is about 26% shorter than the theoretical value 381 ns [13]. As electron correlation effects in two- and three-electron ions are not significant, discrepancies of the type mentioned above arise from blending, cascading contributions or hyperfine quenching. Blending and cascade contributions need to be considered in the analysis of experimental data but do not enter theoretical lifetime calculations, whereas hyperfine corrections have not been incorporated in the theoretical results cited above.

In order to clarify the origin of such discrepancies between theoretical and experimental values, we have undertaken a continuing investigation into He-like  $1s2p {}^3P_2^0$  and Li-like  $1s2s2p {}^4P_{5/2}^0$  level lifetimes in ions having zero nuclear spin. Hyperfine quenching effects are not present in the corresponding ions, thus eliminating a possible source of discrepancy between experimental and theoretical results.

The He-like  $1s2p {}^3P_2^0$  level lifetime in  ${}^{58}\text{Ni}$  ( $I=0$ ) has been determined [14] using the beam-single and beam-two-foil techniques. Our experimental value ( $70 \pm 3$  ps) is in good agreement with theory (70.6 ps) indicating that blending and cascading contributions have been addressed within our experimental technique and analysis. Due to the limited beam travel, we have not been able to determine the  $1s2s2p {}^4P_{5/2}^0$  lifetime in this ion.

In the current study, we proceed and investigate the experimental Li-like  $1s2s2p {}^4P_{5/2}^0$  level lifetime in  ${}^{48}\text{Ti}$ , an ion having zero nuclear spin. The lifetime for this level has been determined by Dohmann *et al.* [15] by a method, based on the Auger electron emission process  $1s2s2p {}^4P_{5/2}^0 - (1s^2 {}^1S_0 + e^-)$ , in which an electrostatic cylindrical mirror analyzer was used. Although this technique is free from satellite blending [1] and the influence of cascades has been taken into account [15], a discrepancy persists between the experimental value ( $236 \pm 12$  ps) of Dohmann *et al.* [15] and theoretical estimates (205 ps) [6] and 212 ps [12] for this  $I=0$  ion. The origin of this discrepancy is addressed within our current experimental approach and analysis. Successful elimination of blending and cascading contributions from a measurement leaves hyperfine quenching as the sole possible source of discrepancy between experimental and theoretical lifetimes in nonzero nuclear-spin He-like and Li-like ions.

## II. EXPERIMENTS AND OBSERVATIONS

The  ${}^{48}_{22}\text{Ti}$  ion beam used in the experiment was obtained from the 15 Unit Double Pelletron accelerator at the Nuclear Science Centre, New Delhi. A collimated, 3-mm-diameter Ti beam was excited by passage through a  $90\text{-}\mu\text{g}/\text{cm}^2$  carbon target. In the two-foil experiment, a  $4\text{-}\mu\text{g}/\text{cm}^2$  thin carbon foil was placed at 2.5 mm upstream from the detector. The experiment was performed using 95 and 143-MeV  ${}^{48}_{22}\text{Ti}$  beams and a setup similar to the one employed in previous studies [1,14]. Details of the current experimental setup, which allows for a longer beam travel, may be found else-

\*Email address: nandi@nsc.ernet.in

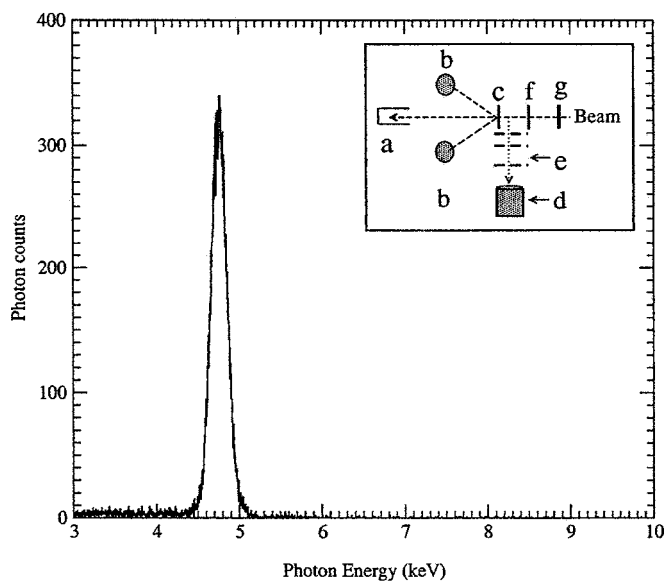


FIG. 1. X-ray spectrum of the 95-MeV  $^{48}\text{Ti}$  beam incident on the  $90\text{-}\mu\text{g}/\text{cm}^2$  carbon foil. Inset shows the schematic of the experimental setup; (a) Faraday cup, (b) Silicon Surface Barrier detector, (c) gold foil, (d) Germanium Ultra Low Energy detector, (e) collimating system, (f) multiple foil holder, (g) movable foil.

where [16]. The spectrum, calibrated using a standard  $^{241}\text{Am}$  x-ray radiation source, exhibits a prominent peak at 4.78 keV (Fig. 1). This peak consists of a blend of transitions from the He-like  $1s2p\ ^3P_0^o$  and  $1s2s\ ^3S_1$  levels and the Li-like  $1s2s2p\ ^4P_{5/2}^o$  level (Table I). This blending is not expected to be resolved by our Germanium ultra-low-energy detector (Canberra, model GUL 0035, energy resolution (full width at half maximum) of 160 eV at the 5.9 keV  $^{55}\text{Fe}$  line). The resolution degrades up to 220 eV for the observed 4.78-keV peak due to Doppler broadening and blending contributions. A typical spectrum is shown in Fig. 1 with the experimental schematic in its inset. The normalized intensity variations of the 4.78-keV line in the single-foil and two-foil measurements at 143 MeV are shown in Fig. 2. In the two-foil measurements, both at 95 MeV and at 143 MeV, the intensity of the line decreases with distance before saturation is reached.

### III. THEORETICAL BACKGROUND

In Fig. 3 we present lifetimes and decay modes for He-like and Li-like  $^{48}\text{Ti}$  levels of interest to this work. Our investigation focuses on the determination of the  $1s2s2p\ ^4P_{5/2}^o$  Li-like level lifetime using its magnetic quadrupole (M2) decay channel to the Li-like ground state (transition energy

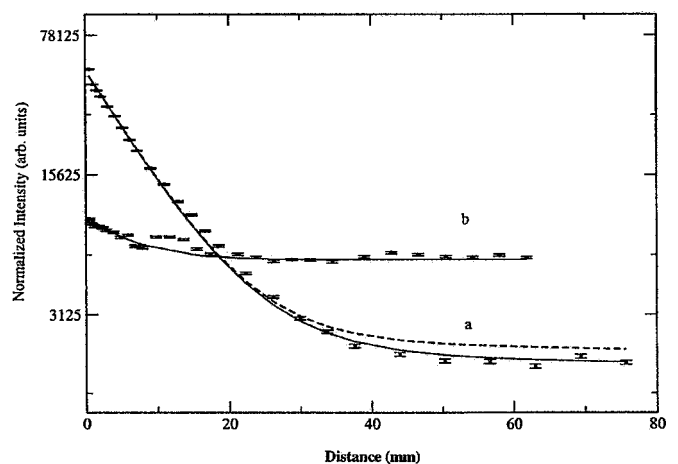


FIG. 2. Normalized intensities for the 4.78-keV line (beam energy 143 MeV) as a function of (a) the distance between the foil and the detector (single-foil) and (b) the separation between the two foils (two-foil experiment, distance between the second foil and the detector fixed to 2.5 mm). Single-foil data, (a) dashed line obtained from a two-exponent fit, solid line from a three-exponent fit using Eq. (2). Two-foil data, (b) solid line obtained by fitting with Eq. (1).

4.69 keV [17]). We note that, for this level, a substantial decay through an autoionization channel (66% branching ratio [6]) is also possible. A theoretical investigation with the code GRASP [17] has revealed the presence of 16 Li-like  $^{48}\text{Ti}$  levels, whose excitation energies with respect to the Li-like ground state lie in the energy range 4.673–4.782 keV. These levels originate from electronic configurations  $1s2s^2\ ^2S_{1/2}$ ,  $1s2p^2\ ^2P_{1/2,3/2}$ ,  $^4P_{1/2,3/2,5/2}$ ,  $^2D_{3/2,5/2}$ ,  $^2S_{1/2}$ ,  $1s2s2p\ ^4P_{1/2,3/2,5/2}^o$  and  $^2P_{1/2,3/2}^o$ . The even parity levels in the list mentioned above are linked to the Li-like ground state with low radiative transition probabilities [17] and do not contribute to the 4.78-keV line. With the exception of  $1s2s2p\ ^4P_{5/2}^o$ , the E1 transitions linking the odd parity levels to the Li-like ground state are significant [6,17]. These levels have very short lifetimes and need not therefore be considered further. As a result, the only Li-like level that will be considered in the analysis of the 4.78-keV line is the  $1s2s2p\ ^4P_{5/2}^o$  level ( $1s2s2p\ ^4P_{5/2}^o - 1s^22s^2S_{1/2}$  M2 transition, x-ray emission rate  $1.6 \times 10^9\ \text{s}^{-1}$  [6]).

We note further that a number of He-like levels (cf. Fig. 3) may also in principle contribute to the 4.78 keV line. The He-like  $1s2p\ ^3P_0^o$  level decays through an M2 transition to the ground state  $1s^2\ ^1S_0$  by emitting a 4.734-keV x-ray photon. The  $1s2s\ ^1S_0$  level, on the other hand, decays through a two-photon process [18], whereas the  $1s2p\ ^3P_0^o$  level decays to the  $1s2s\ ^3S_1$  level through an E1 transition in the vacuum

TABLE I. Theoretical lifetimes and transition energies for the levels that may contribute to the 4.78-keV line.

Ion	Transition	Energy (keV)	Lifetime
$\text{Ti}^{20+}$	$1s^2\ ^1S_0 - 1s2p\ ^3P_0^o$	4.734 [21]	422 ps [5]
$\text{Ti}^{20+}$	$1s^2\ ^1S_0 - 1s2s\ ^3S_1$	4.702 [21]	26.6 ns [5]
$\text{Ti}^{19+}$	$1s^22s\ ^2S_{1/2} - 1s2s2p\ ^4P_{5/2}^o$	4.690 [17]	205 ps [6], 212 ps [12]

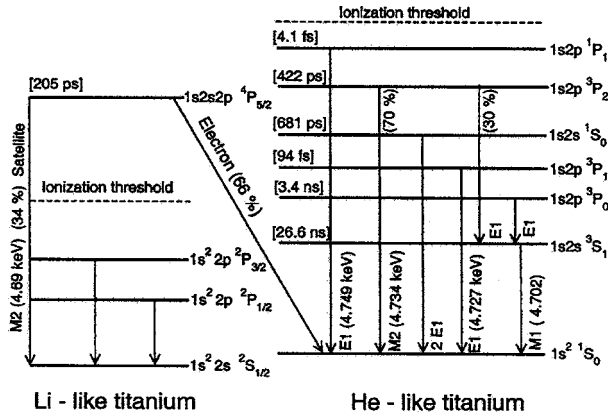


FIG. 3. Theoretical transition energies, lifetimes, and branching ratios in He-like [5,17,18,21] and Li-like [6,17] titanium.

ultraviolet region [5]. These two levels do not therefore directly contribute to the 4.78-keV line. The  $1s2p^1P_1^o$  and  $1s2p^3P_1^o$  levels, with lifetimes of the order of fs [5], do not contribute to the decay curves shown in Fig. 2. The only other He-like level that needs to be considered is  $1s2s^3S_1$  (lifetime 26.6 ns [5], transition energy 4.702 keV [19]). The Li-like  $1s2s2p^4P_{5/2}^o$  and the He-like  $1s2p^3P_2^o$  and  $1s2s^3S_1$  levels lie within 50 eV. Since contributions from these levels to the 4.78-keV line cannot be resolved by the x-ray detector used in our experiment, all three levels were taken into consideration in the analysis of the 4.78-keV data. The H-like  $2s^2S_{1/2}$  level (lifetime 1.014 ns, Ref. [20]) decays mainly through a two-photon process to the H-like ground state. For this level, an M1 decay by emission of a 4.966-keV photon [29] is also possible (decay rate  $6.82 \times 10^7 \text{ s}^{-1}$  [20]). This line, however, has not been observed in the spectrum, implying that the H-like  $2s^2S_{1/2}$  level is not promptly populated in our experiment. None of the Be- and B-like  $^{48}_{22}\text{Ti}$  ions contain levels that meet the transition energy as well as the lifetime requirements [17] imposed by the 4.78-keV peak.

TABLE II. Lifetimes for the Li-like  $^{48}_{22}\text{Ti}$   $1s2s2p^4P_{5/2}^o$  and He-like  $^{48}_{22}\text{Ti}$   $1s2p^3P_2^o$  levels. (a) Single-foil data fitted with two exponents. One exponent represents an effective lifetime ( $\tau_s$ ) for both  $1s2p^3P_2^o$  and  $1s2s2p^4P_{5/2}^o$  levels, the other (fixed) the  $1s2s^3S_1$  lifetime. (b) Two-foil data fitted with Eq. (1) (see text). The  $1s2p^3P_2^o$  level lifetime  $\tau_2$  is determined by fixing  $\tau_1$  to the single-foil result  $\tau_s$  and  $\tau_3$  to the  $1s2s^3S_1$  lifetime. (c) Single-foil data fitted with three exponents [Eq. (2), the lifetime of  $1s2s2p^4P_{5/2}^o$  was varied and lifetimes of  $1s2p^3P_2^o$  and  $1s2s^3S_1$  were fixed to 404 ps and 26.6 ns, respectively].

Upper level	Beam energy (MeV)	Experiment This work ps	Experiment Other work ps	Theoretical lifetime ps
All (unresolved)	95	$265 \pm 9(\tau_s)^a$		$290 \pm 29$ [26]
All (unresolved)	143	$310 \pm 6(\tau_s)^a$		$328 \pm 33$ [26]
$1s2p^3P_2^o$	95	$419 \pm 20(\tau_2)^b$		
$1s2p^3P_2^o$	143	$389 \pm 18(\tau_2)^b$		
$1s2s2p^4P_{5/2}^o$	95	$193 \pm 13(\tau_1)^c$		
$1s2s2p^4P_{5/2}^o$	143	$228 \pm 14(\tau_1)^c$		
$1s2s2p^4P_{5/2}^o$	average	$210.5 \pm 13.5$	$236 \pm 12$ [15], $200 \pm 12$ [28]	$212$ [12], $205$ [6]
$1s2p^3P_2^o$	average	$404 \pm 19$	$404 \pm 40$ [15]	$422$ [5]

#### IV. DATA ANALYSIS, RESULTS, AND DISCUSSION

The charge state fractions for the  $^{48}_{22}\text{Ti}$  beams used in this work have been obtained with the code ETACHA [22]. Energy losses in the foil were taken into account in the charge-state fraction calculation using the code SRIM [23]. Results of experiments performed at GANIL with projectile energies in the range 10–80 MeV/A [22] agree with theoretical charge-state fractions obtained with the code ETACHA. It has been further noted (Table 2 in Ref. [14]) that ETACHA predictions are consistent with the use of low energy (1.6–2.5 MeV/A) Cl beams in the investigation of He-like  $1s2p^3P_0^o - 1s2s^3S_1$  and  $1s2p^3P_0^o - 1s2s^3S_1$  transitions [24]. Although no charge-state fraction data are available for  $^{48}_{22}\text{Ti}$  beams in the range 2–5 MeV/A, we note that Dohmann *et al.* [15] used rather low-energy beams (3.6 and 5.0 MeV/A) in their investigation of He- and Li-like  $^{48}_{22}\text{Ti}$  lifetimes. This is again consistent with the ETACHA prediction that, at low beam energies, and for a carbon foil of similar thickness ( $90 \mu\text{g}/\text{cm}^2$ ) to those used in Ref. [15] ( $100\text{--}160 \mu\text{g}/\text{cm}^2$ ), He-like and Li-like levels are indeed significantly populated in the post-foil beam. We further note that the use of 216-MeV  $\text{Ti}^{9+}$  beams [25] in the measurement of the  $1s2s^3S_1 - 1s2p^3P_2^o$  transition energy in He-like  $\text{Ti}^{20+}$  is also consistent with ETACHA charge-state fraction predictions.

The decay curve generated from the single-foil experiment at 143 MeV [Fig. 2(a)] demonstrates the presence of two components. The first component is linked to an “effective” lifetime  $\tau_s$  associated with the  $1s2p^3P_2^o$  and  $1s2s2p^4P_{5/2}^o$  levels, whose theoretical lifetimes lie within a factor of 2. The second component is associated with the (longer-living)  $1s2s^3S_1$  level, for which reliable theoretical lifetime values are available. We therefore used the theoretical  $1s2s^3S_1$  lifetime value (Table I) in the two-component fit of the single-foil data. The lifetime  $\tau_s$ , determined in this way for the first component (Table II), is  $310 \pm 6$  ps (beam energy 143 MeV) and  $265 \pm 9$  ps (beam energy 95 MeV). These values are larger than the theoretical lifetime of the

TABLE III. Correspondence between processes occurring at the second foil and various terms in Eq. (1) (see text for details).

Levels before the second foil	Levels after the second foil	Intensity component
$1s^2$	All excited levels giving rise to unresolved transitions in He- and Li-like ions	$I_1$
(i) $1s2s\ ^3S_1$ (arising from $1s2p\ ^3P_2^o$ ) and (ii) $1s2p\ ^3P_2^o$	$1s2s2p\ ^4P_{5/2}^o$ (populated by electron capture or intrashell transition followed by electron capture)	$I_2$
$1s2s\ ^3S_1$	$1s2s2p\ ^4P_{5/2}^o$ (populated by electron capture or intrashell transition followed by electron capture)	$I_3$

$1s2s2p\ ^4P_{5/2}^o$  level (205 ps) and lower than that of the  $1s2p\ ^3P_2^o$  level (422 ps), an indication that both levels contribute to this line. This is consistent with ETACHA predictions for the charge-state fractions of the post-foil beam. Thus the value  $\tau_s$  represents an effective lifetime for both  $1s2p\ ^3P_2^o$  and  $1s2s2p\ ^4P_{5/2}^o$  levels. The values for this effective lifetime are also in good agreement with estimates obtained from a semiempirical formula (Table II in Ref. [26]).

The curve constructed from the two-foil measurement at 143 MeV [Fig. 2(b)] decreases at first and reaches saturation as the distance between the two foils increases. In order to analyze the two-foil data, we followed a similar procedure to that employed in earlier studies [1,14] and fitted the data using the following equation:

$$I(x) = I_1 e^{-x/\nu\tau_1} + I_2 (1 - e^{-x/\nu\tau_2}) + I_3 (1 - e^{-x/\nu\tau_3}). \quad (1)$$

Here,  $I(x)$  is the intensity as a function of the distance  $x$  between the two foils. The growing components are associated with  $1s2s2p\ ^4P_{5/2}^o$  populated as a result of the presence of  $1s2p\ ^3P_2^o$  ( $\tau_2$ ) and  $1s2s\ ^3S_1$  ( $\tau_3$ ) levels.

To relate the components in Eq. (1) with processes occurring at the second foil, we introduce a plausible model, summarized in Table III. Intensity  $I_1$  is associated with levels generated from  $1s^2$  that give rise to unresolved transitions contributing to the 4.78-keV line.  $I_2$  is associated with  $1s2s2p\ ^4P_{5/2}^o$ , originating from  $1s2p\ ^3P_2^o$  levels.  $I_3$  is due to  $1s2s2p\ ^4P_{5/2}^o$  originating from  $1s2s\ ^3S_1$  levels.  $1s2s2p\ ^4P_{5/2}^o$  levels in  $I_2$  and  $I_3$  are populated through electron capture or through intrashell transitions followed by electron capture at the second foil.

It is worth noting that a humplike structure is present in the range 10–20 mm [Fig. 2(b), two-foil data]. This feature is due to delayed cascade feeding of H-like Ti  $2s\ ^2S_{1/2}$  and  $2p\ ^2P_{1/2,3/2}$  levels [27] from high- $n$  Rydberg states, during the beam flight between the two foils. Further, these states may generate He-like  $1s2p\ ^3P_2^o$  and  $1s2s\ ^3S_1$  states through electron capture processes on colliding with the second foil. Similar features have also been observed in other two-foil experiments and are being thoroughly investigated.

A least-square fit of the two-foil data at 143 MeV using Eq. (1) was then performed, excluding the data in the 10–20

mm range. In the fitting procedure, the effective lifetime  $\tau_1$  was fixed to the value  $\tau_s$  ( $310 \pm 6$  ps) obtained from the single-foil measurement. This value has been associated with contributions from both  $1s2p\ ^3P_2^o$  and  $1s2s2p\ ^4P_{5/2}^o$  levels. The value of  $\tau_3$  was fixed to 26.6 ns, the theoretical  $1s2s\ ^3S_1$  level lifetime. The decay time  $\tau_2$ , associated with the  $1s2p\ ^3P_2^o$  lifetime, is then determined to be  $389 \pm 18$  ps (Table II, beam energy 143 MeV). The 95-MeV data were analyzed in a similar manner to yield a value of  $419 \pm 20$  ps for  $\tau_2$  (Table II, beam energy 95 MeV). The average lifetime ( $\tau_2$ ,  $404 \pm 19$  ps) of the  $1s2p\ ^3P_2^o$  level at the two beam energies is consistent with an earlier experimental result ( $404 \pm 40$  ps) in which a flat crystal spectrometer was used [15]. This result is also consistent with the theoretical value (422 ps, Ref. [5]), calculated within the relativistic random-phase approximation.

Finally, in order to disentangle the contribution of the  $1s2p\ ^3P_2^o$  level from the effective lifetime  $\tau_s$ , we employ, in place of the first component in the earlier fit of the single-foil data, two exponents, as follows:

$$I(x) = [I'_1 e^{-x/\nu\tau'_1} + I''_1 e^{-x/\nu\tau''_1}] + I_2 e^{-x/\nu\tau_2}. \quad (2)$$

Here,  $\tau'_1$  represents the Li-like  $1s2s2p\ ^4P_{5/2}^o$  level lifetime and  $\tau''_1$  the He-like  $1s2p\ ^3P_2^o$  level lifetime. In the fitting,  $\tau_2$  was fixed to 26.6 ns,  $I_2$  was fixed to the value obtained from the two-exponent fit of the single-foil data and  $\tau''_1$  was kept fixed at the average  $1s2p\ ^3P_2^o$  level lifetime value  $404 \pm 19$  ps (Table II). The ratio  $I'_1 : I''_1$  was set to the post-foil charge-state fraction ratio of Li-like to He-like  $^{48}_{22}\text{Ti}$  ions. A value of  $228 \pm 14$  ps was thus obtained for  $\tau'_1$ , associated with the  $1s2s2p\ ^4P_{5/2}^o$  level lifetime. Single-foil data at 95 MeV were also fitted in this manner to yield a value ( $193 \pm 13$  ps, Table II) for the  $1s2s2p\ ^4P_{5/2}^o$  level lifetime. The average  $1s2s2p\ ^4P_{5/2}^o$  level lifetime from the measurements at the two beam energies is  $210.5 \pm 13.5$  ps (Table II). This value is lower than that determined in an earlier experimental study ( $236 \pm 12$  ps) [15] and close to our recent beam two-foil measurement ( $200 \pm 12$  ps) in which a different approach was used [28]. The  $1s2s2p\ ^4P_{5/2}^o$  level lifetime, determined in the current study, is very close to the theoretical value of 212 ps [12] calculated within a relativistic Hartee-Fock model. A

relativistic calculation in the intermediate-coupling scheme [6], in which Dirac-Hartree-Slater wave functions and the Møller two-electron operator were used, gives a value (205 ps) that is also within the uncertainty range of our present result.

The analysis followed in the present study closely resembles that in our earlier work [1,14]. We note, however, that, this time, the  $1s2s\ ^3S_1$  level must be considered explicitly in the equations that are used in the fitting procedure. This is due to the fact that our present experimental setup allows for a considerably longer beam travel than our previous studies.

The velocity of the post-foil beam was calculated from the beam energy at the exit of the foil. The beam energy was calibrated with nuclear resonances. Electronic and nuclear energy losses in the foil were taken into account using the code SRIM [23]. The uncertainty in the beam velocity is less than 1%. In order to minimize the Doppler effect in the measurement, the x-ray detector was placed at  $90^\circ \pm 1^\circ$  with respect to the beam direction. The foils were made parallel by maximizing the capacitance at a certain smallest distance. Errors in lifetime values arise in this work from statistical uncertainties ( $\sigma$ ) and from the approximations introduced in the fitting procedures. Up to  $2\sigma$  uncertainties were introduced in the intensities so as to include all sources of errors which result in the reduced  $\chi^2$  value close to unity. The uncertainty in each measurement represents one standard deviation in the lifetime value. The average lifetime quoted in this work represents a mean of the two measured values  $\Delta_1, \Delta_2$  at

different beam energies. The reported uncertainty is the standard error ( $\sqrt{\Delta_1^2 + \Delta_2^2}/2$ ).

## V. CONCLUSION

In this work, we have determined the Li-like  $^{48}\text{Ti}\ 1s2s2p\ ^4P_{5/2}^o$  level lifetime, through its M2 x-ray decay channel to the Li-like ground state. Theoretical estimates for this lifetime lie within the uncertainty bounds of our experimental result. A two standard-deviation difference between a previous experimental result ( $236 \pm 12$  ps [15]) and theoretical predictions (205 ps [6] and 212 ps [12]) does not therefore arise within our measurements and subsequent analysis. Experimental He-like  $1s2p\ ^3P_2^o$  and Li-like  $1s2s2p\ ^4P_{5/2}^o$  level lifetimes for hyperfine quenching free ions, obtained with the current experimental setup and analysis, are in good agreement with theoretical predictions. The origin of the discrepancies between experimental and theoretical  $1s2s2p\ ^4P_{5/2}^o$  level lifetimes in Li-like Cl [10,11] and V [1] is still under investigation and is expected to be addressed by experiments capable of resolving the Li-like  $1s2s2p\ ^4P_{5/2}^o \rightarrow 1s^22s\ ^2S_{1/2}$  and the He-like  $1s2p\ ^3P_2^o \rightarrow 1s^2\ ^1S_0$  lines.

## ACKNOWLEDGMENTS

We thank the Pelletron staff at IUAC for providing stable ion beams. We also gratefully acknowledge useful discussions with B. Mukherjee and G. K. Padmashree during the preparation of the manuscript.

- 
- [1] T. Nandi *et al.*, Phys. Rev. A **66**, 052510 (2002).  
 [2] L. Kay, Phys. Lett. **5**, 36 (1963).  
 [3] S. Cheng *et al.*, Phys. Rev. A **50**, 2197 (1994).  
 [4] H. Gould, R. Marrus, and P. J. Mohr, Phys. Rev. Lett. **33**, 676 (1974).  
 [5] C. D. Lin, W. R. Johnson, and A. Dalgarno, Phys. Rev. A **15**, 154 (1977).  
 [6] M. H. Chen, B. Crasemann, and H. Mark, Phys. Rev. A **24**, 1852 (1981).  
 [7] U. I. Safronova, V. S. Senashenko, and I. A. Shavtvalishvili, Physica A **12**, 13 (1977).  
 [8] K. Cheng, C. Lin, and W. R. Johnson, Phys. Lett. A **48**, 437 (1974).  
 [9] R. H. Garstang, J. Opt. Soc. Am. **52**, 845 (1962). (The hyperfine interaction causes a small admixture between atomic states of the same electronic configuration characterized by different total electronic angular momentum. As a result, forbidden E1 transitions are now possible. The hyperfine-induced additional branches cause a reduction of the lifetimes of some metastable levels, an effect known as hyperfine quenching.)  
 [10] C. L. Cocke, B. Curnutte, and J. R. McDonald, Nucl. Instrum. Methods **110**, 493 (1973).  
 [11] I. A. Sellin, D. J. Pegg, P. M. Griffin, and W. W. Smith, Phys. Rev. Lett. **28**, 1229 (1972).  
 [12] C. P. Bhalla and T. W. Tunnell, Z. Phys. A **303**, 199 (1981).  
 [13] C. L. Cocke, B. Curnutte, and R. Randall, Phys. Rev. Lett. **31**, 507 (1973).  
 [14] T. Nandi *et al.*, J. Phys. B **37**, 703 (2004).  
 [15] H. D. Dohmann, R. Mann, and E. Pfeng, Z. Phys. A **309**, 101 (1982).  
 [16] Nissar Ahmad *et al.* (unpublished).  
 [17] I. P. Grant, C. F. Fischer, and F. A. Parpia, GRASP-1992 (private communication).  
 [18] G. W. F. Drake, Phys. Rev. A **34**, 2871 (1986).  
 [19] G. W. Drake, Can. J. Phys. **66**, 586 (1988).  
 [20] F. A. Parpia and W. R. Johnson, Phys. Rev. A **26**, 1142 (1982).  
 [21] J. Sugar and C. Corliss, J. Phys. Chem. Ref. Data **14**, 581 (1985), Supplement No. 2.  
 [22] J. P. Rozet, C. Stéphan, and D. Vernhet, Nucl. Instrum. Methods Phys. Res. B **107**, 67 (1996).  
 [23] J. F. Zeigler, SRIM-2000 computer code (private communication).  
 [24] H. G. Berry, R. DeSerio, and A. E. Livingston, Phys. Rev. Lett. **41**, 1652 (1978).  
 [25] E. J. Galvez *et al.*, Phys. Rev. A **33**, 3667 (1986).  
 [26] T. Nandi, Indian J. Phys., B **76**, 407 (2004).  
 [27] T. Nandhi *et al.* (unpublished).  
 [28] T. Nandi, Nissar Ahmad, and A. A. Wani, Phys. Rev. A **72**, 022711 (2005).  
 [29] P. J. Mohr, At. Data Nucl. Data Tables **29**, 453 (1983).